[CANCER RESEARCH 64, 3885–3891, June 1, 2004]

Cyclin-Dependent Kinase Inhibition by the KLF6 Tumor Suppressor Protein through Interaction with Cyclin D1

Sharon Benzeno,[1] Goutham Narla,[1] Jorge Allina,[1] George Z. Cheng,[1] Helen L. Reeves,[1] Michaela S. Banck,[1,2] Joseph A. Odin,[1] J. Alan Diehl,[3] Doris Germain,[2] Scott L. Friedman[1]

Divisions of [1]Liver Diseases and [2]Hematology-Oncology, Department of Medicine, Mount Sinai School of Medicine, New York, New York, and [3]Abramson Family Cancer Research Institute, University of Pennsylvania Cancer Center, Philadelphia, Pennsylvania

ABSTRACT

Kruppel-like factor 6 (KLF6) is a tumor suppressor gene inactivated in prostate and colon cancers, as well as in astrocytic gliomas. Here, we establish that KLF6 mediates growth inhibition through an interaction with cyclin D1, leading to reduced phosphorylation of the retinoblastoma protein (Rb) at Ser^{795}. Furthermore, introduction of KLF6 disrupts cyclin D1-cyclin-dependent kinase (cdk) 4 complexes and forces the redistribution of $p21^{Cip/Kip}$ onto cdk2, which promotes G_1 cell cycle arrest. Our data suggest that KLF6 converges with the Rb pathway to inhibit cyclin D1/cdk4 activity, resulting in growth suppression.

INTRODUCTION

Kruppel-like factor 6 (KLF6) is a zinc finger tumor suppressor protein inactivated in sporadic prostate (1, 2) and colon cancers (3) and astrocytic gliomas (4). Furthermore, KLF6 promoter methylation has been identified in esophageal cancer cells (5). KLF6 is a member of a growing family of transcription factors that share a COOH-terminal C_2H_2 DNA binding domain but have widely divergent NH_2-terminal activation domains (6, 7). Growth suppressive activity of KLF6 is linked to p53-independent transactivation of $p21^{WAF1/Cip1}$, a key cyclin-dependent kinase (cdk) inhibitor (1).

Some tumor-derived mutants of KLF6 have been identified that can no longer transactivate $p21^{WAF1/Cip1}$ (1). Several other KLF6 mutants, however, preserve p21 transactivation activity, yet these still fail to suppress growth (3). This finding suggests that KLF6 might provoke growth arrest through functionally parallel circuits, a property that is typical of other tumor suppressor genes such as p53 (8–10) or p16 (11).

Direct interaction with cell cycle regulators characterizes growth suppression by several tumor suppressor genes. The INK4a gene, for example, encodes the $p16^{INK4a}$ tumor suppressor protein that binds to cdk4 and alters the binding of D-type cyclins, thus, reducing the kinase's affinity to ATP (12). By preventing the formation of cdk4/6-cyclin D complexes, INK4 proteins force the redistribution of the Cip/Kip family of inhibitors (*e.g.*, p21) from cdk4/6-cyclin D1 holoenzymes toward binding and down-regulating the kinase activity of cdk2-cyclin E complexes, thereby blocking exit from G_1 (12).

Evasion of the cyclin-dependent and the retinoblastoma (Rb) pathways are common alternative mechanisms by which tumor cells escape the G_1 restriction point (13). Cyclin D1/cdk complexes are part of a more extensive cell cycle regulatory pathway that includes the Rb protein, a nuclear phosphoprotein that is differentially phosphorylated on serine and threonine residues during the cell cycle. Phosphorylation of Rb by cdks leads to S-phase entry and marks the irreversible commitment of the cell to exit the G_1 (resting) phase. Key to the control of cell growth at this G_1-S junction is the cyclin D-$p16^{INK4a}$-Rb pathway.

Loss of cell cycle control is a common event in malignancies (14). The D-type cyclins (D1, D2, D3) are responsible for integrating extracellular signals into the cell (14). The cyclinD1/CCND1 oncogene (PRAD1), for example, is amplified in a number of primary cancers. Cyclin D1 overexpression, however, has been detected at a higher frequency than can be accounted for by gene amplification alone (15). Thus, mechanisms other than DNA amplification may lead to deregulated expression of cyclin D1 in cancer. Additionally, because deregulated expression of cyclin D1 directly contributes to tumorigenesis in a number of animal model systems (16, 17), inhibition of cyclin D1 function may be an important target of cancer prevention and therapy (18).

Because the KLF6 sequence predicts consensus sites for both a cdk phosphorylation site at Ser^{171} (19) and a proximal cyclin E/A consensus binding site at the COOH terminus ('ZRXL' motif, Z = basic residue, at amino acids 279–283), we have explored the possibility that KLF6 interacts directly with cell cycle components. Here, we describe an interaction between the tumor suppressor protein KLF6 and cyclin D1, defining a novel mechanism of KLF6-mediated growth suppression and identifying this protein as a putative cdk inhibitor (CKI).

MATERIALS AND METHODS

Cell Lines. Cell lines were obtained from the American Tissue Culture Collection. 293T, Hep3B, and HCT116 cell lines were cultured in DMEM (BioWhittaker) supplemented with 10% (v/v) fetal bovine serum (Hyclone), antibiotics (penicillin, streptomycin 100 mg/ml; Cellgro), and L-glutamine (30 mg/ml). The NIH3T3 cell line was cultured in DMEM supplemented with calf serum. All cell lines were grown in 5% CO_2 at 37°C.

Plasmids. pCIneo-KLF6 (human) expression vector was constructed as previously described (19) by fusing a full-length KLF6 cDNA cloned into the *Eco*RI and *Xba*I sites of the pCIneo vector. FLAG-tagged full-length KLF6 was constructed by restriction digest and subcloning into a pcDNA3 vector expressing the M5 (FLAG) epitope at the NH_2 terminus. The cyclin D1 expression vector was a gift from Dr. Charles Sherr (St. Jude Cancer Center, Nashville, TN).

Retrovirus Construction, Propagation, and Infection. Human KLF6 cDNA (19) was cloned into pBabe-puro expression vector. Constructs containing the KLF6 sequence (pBabe-KLF6) or empty vector control (pBabe) were transiently transfected by lipofection (Lipofectamine 2000; Invitrogen) into 50% confluent Phoenix A packaging cells producing nonreplicating forms of amphotropic virus [a generous gift from Dr. Gary Nolan (Stanford, CA)] in 15-cm plates used according to the manufacturer's protocol. Transfection medium was removed after 4 h and replaced with fresh medium. The supernatant from the packaging cells was collected three times daily for 3 days after transfection and filtered through a 0.45-μm membrane to remove contaminating packaging cells. For infection, 4×10^4 cells HCT116 target cells were seeded in 10-cm plates and were exposed to 5 ml of viral supernatant containing viable virus in the presence of 8 μg/ml Polybrene (Sigma, St. Louis, MO) for 4 h, twice in succession. Depending on the experiment, HCT116 cells were selected with 5 μg/ml puromycin.

Received 9/5/03; revised 3/19/04; accepted 3/19/04.

Grant support: NIH Grants DK37340 (S. Friedman) and T32DK07832 (J. Odin), the Howard Hughes Medical Institute (G. Narla), the American Liver Foundation (G. Narla and G. Cheng), and the Revson Foundation (M. Banck) and American Society of Clinical Oncology Young Investigator Award (M. Banck).

The costs of publication of this article were defrayed in part by the payment of page charges. This article must therefore be hereby marked *advertisement* in accordance with 18 U.S.C. Section 1734 solely to indicate this fact.

Requests for reprints: Scott L. Friedman, Box 1123, Mount Sinai School of Medicine, 1425 Madison Avenue, Room 1170F, New York, NY 10029. Phone: (212) 659-9501; Fax: (212) 849-2574; E-mail: Scott.Friedman@mssm.edu.

Antibodies. The polyclonal anti-KLF6 (R-173), the polyclonal anti-cdk4, and the monoclonal anti-cyclin D1 antibodies were obtained from Santa Cruz Biotechnology. The anti-KLF6 monoclonal antibody was generated in the monoclonal antibody core facility at Mount Sinai School of Medicine using as the immunogen the NH_2-terminal transactivation domain (residue 1–201) expressed as a GST-fusion protein. The anti-Rb and anti-pSer795-Rb antibodies were obtained from Cell Signaling (Beverly, MA). The anti-HA, anti-FLAG, and anti-β-tubulin antibodies were obtained from Sigma.

Western Blot Analysis. Unless otherwise indicated, whole cell protein extracts were obtained by lysing cells in lysis buffer [50 mM HEPES (pH 7.5), 150 mM NaCl, 1 mM EDTA, 0.1% NP40, 10% glycerol, 20 mM β-glycerophosphate, 0.1 mM sodium vanadate, 1 mM NaF, 1 mM phenylmethylsulfonyl fluoride, and 1 protease inhibitor tablet/10 ml buffer]. For Western blot, 30–50 μg of total cell extracts were resolved on either 10 or 12% SDS-PAGE. After transfer onto nitrocellulose membranes, proteins of interest were detected by incubating with primary antibodies [α-KLF6-1:250 (polyclonal), α-cyclin D1-1:250, cdk4-1:250, α-Rb- and α-pSer^{795}-Rb-1:1000, and α-β tubulin-1:1000] and processed by the standard enhanced chemiluminescence detection method under conditions recommended by the manufacturer (Amersham). Nitrocellulose membranes were then subjected to autoradiography.

For repeated blots using the same membranes, they were stripped and reprobed after being submerged in stripping buffer [100 mM β-mercaptoethanol, 2% SDS, 62.5 mM Tris-HCl (pH 6.7)] and incubated at 50°C for 30–45 min with shaking approximately every 10 min. The membranes were then washed twice for 10 min in Tris-buffered saline-Tween at room temperature using large volumes of wash buffer. After blocking for 1 h at room temperature in 5% dry milk/Tris-buffered saline-Tween, immunodetection was performed as described above.

Immunoprecipitation. All protein extracts were precleared by nutation in the presence of protein G-agarose beads and a corresponding control immunoglobulin for 30 min at 4°C. Supernatant was then collected, and 20–40 μl of either protein G-, HA-, or M2-FLAG-agarose beads were added for immunoprecipitation with nutation overnight at 4°C of the desired protein. The next day, beads were washed four times with lysis buffer, and proteins were subsequently boiled off the beads in 1× SDS protein loading buffer and separated on SDS-PAGE gels for subsequent Western analysis. The same procedure was used for immunoprecipitation of endogenous KLF6 from NIH3T3, Hep3B, and HCT116 cells. Endogenous KLF6 was incubated for 1 h with a monoclonal antibody specific to KLF6 (2A2) before protein G-agarose beads were added, and immunoprecipitation followed with nutation overnight at 4°C.

Nonradioactive cdk4 Immunoprecipitation Kinase Assay. Immunoprecipitation/kinase assays were performed using a modification of the method described by Jinno *et al.* (20). In brief, 200–700 μg of whole cell extracts were immunoprecipitated with antibody to cdk4 (Santa Cruz Biotechnology, Santa Cruz, CA) or a control antibody (as described in preceding section). Next, beads were washed twice with lysis buffer and twice in 1× Rb kinase buffer before they were incubated in Rb kinase reaction buffer [50 mM HEPES (pH 7.5), 1 mM EGTA, 10 mM KCl, 10 mM $MgCl_2$, 1 mM DTT, and 10 mM ATP] containing 0.5 μg of recombinant Rb protein (QED Biosciences, San Diego, CA). The reaction mixture was left for 30 min at 30°C with gentle shaking and was neutralized by addition of 50 μl of 1× SDS protein loading buffer before Western analysis. For this assay, antibody recognizing Ser^{795}-phosphorylated forms of Rb (Cell Signaling) was used. This site on Rb is efficiently phosphorylated by cyclin D/cdk4 complexes (21) and yields a single band on Western blot, rather than the characteristic smear when multiple isoforms are detected using total Rb antibody.

Transfection. Transient transfections were performed using Lipofectamine 2000 reagent (Invitrogen). Lipofectamine was removed 4–6 h after transfection and cells were allowed to recover overnight in complete 10% fetal bovine serum medium. Twenty-four h after transfection, cells were washed three times with cold PBS, and cell lysates were prepared.

Small Interfering RNA (siRNA) KLF6 Silencing. The specific sequence of small interference RNA for KLF6 consists of a 19-nucleotide (nt) sequence of exon 2 separated by a 9-nt spacer from the reverse complement of the same sequence (sense 5′-GGAGAAAAGCCUUACAGAUTT-3′ and antisense 3′-TTCCUCUUUUCGGAAUGUCUA5-′). The oligonucleotide was cloned and expressed in a pSuper plasmid (22). The resulting pSuper-KLF6 plasmid was transfected into HCT116 cells, and cells were harvested 24 h after transfection. The pSuper vector expressing an irrelevant protein, pSuper-Luciferase (pLUC), was used as a control.

Real-Time Quantitative-PCR. Total cellular RNA was extracted using RNeasy Mini kit (Qiagen). All RNA was treated with DNAse (Qiagen). A total of 1 μg of RNA was reverse transcribed/reaction using first-strand cDNA synthesis with random primers (Promega). Real-time quantitative-PCR was performed using the following PCR primers on an ABI PRISM 7900HT Sequence Detection System (Applied Biosystems): KLF6 forward: 5′-CGGACGCACACAGGAGAAAA-3′ and KLF6 reverse: 5′-CGGTGTGCTTTCGGAAGT G-3′; GAPDH forward: 5′-CAATGACCCCTTCATTGACC-3′ and GAPDH reverse: 5′-GATCTCGCTCCTGGAAGATG-3′. All experiments were done in triplicates and normalized to glyceraldehyde-3-phosphate dehydrogenase. Fluorescent signals were analyzed during each of ~20 cycles consisting of denaturation (95°C, 15 s), annealing (56°C, 15 s), and extension (72°C, 40 s). Relative quantitation was calculated using the comparative threshold cycle method (C_T; as described in the User Bulletin no. 2, ABI PRISM 7900HT Sequence Detection System). C_T indicates the fractional cycle number at which the amplified gene amounts to a fixed threshold within the linear phase of amplification. Median C_T of triplicate measurements were used to calculate ΔC_T as the C_T of KLF6 and glyceraldehyde-3-phosphate dehydrogenase. ΔC_T for each sample was compared with ΔC_T for the control expressed as $\Delta\Delta C_T$. Relative quantification was expressed as fold-change of KLF6 expression compared with control condition with the formula $2^{-\Delta\Delta CT}$. Denaturing curves and agarose gel electrophoresis of PCR product for KLF6 and the housekeeping gene were used to confirm homogeneity of the DNA products.

Proliferation Analysis. Proliferation was measured by estimating [^{3}H]thymidine incorporation into DNA. A total of 100–150 × 10^4 HCT116 cells was seeded in 12-well plates for transfection the next day. Cells were transfected for 4–6 h with 1.6 μg of wild-type KLF6, p16^{INK4a} or empty vector DNA as a control and left to recover from the transfection overnight in medium containing 10% fetal bovine serum. The next day, the cells were starved for 24 h in 0.2% fetal bovine serum. [^{3}H]Thymidine was added at 1 μCi/ml (1 μCi = 37kBq; in dilution with cold thymidine) during the last 2 h of serum starvation. After 24 h of serum starvation, cells were washed three times with ice-cold PBS and fixed in cold methanol for 30 min at 4°C. Methanol was subsequently removed, and the cells were allowed to air-dry for 3–5 min. Next, cells were solubilized in 0.25% sodium hydroxide/0.25% SDS and neutralized with hydrochloric acid (1N). Disintegrations/min were estimated in a liquid scintillation counter.

Cell Cycle Analysis by Fluorescence-Activated Cell Sorting. For fluorescence-activated cell sorting analysis, cells were washed twice in 1× PBS, trypsinized with 1 ml of trypsin-EDTA, centrifuged, and washed in 1× PBS once more. Next, cells were resuspended in 250 μl of 1× PBS and 750 μl of prechilled (−20°C) 100% ethanol, which was added dropwise while cells were gently vortexed. To allow for proper fixation, cells were kept on ice for at least 30 min, then centrifuged at 1000 rpm for 10 min at 4°C, washed twice in PBS, and resuspended in 1 ml of PBS and RNaseA treated for 30 min in a 37°C water bath. Finally, before fluorescence-activated cell sorting analysis, cells were incubated with propidium iodide and scanned by flow cytometry using a Becton-Dickinson Excalibur.

Densitometric Analysis. Enhanced chemiluminescent images of immunoblots were analyzed by scanning densitometry and quantified with the BIOQUANT NOVA imaging system (BIOQUANT NOVA PRIME Measurement Software). Values are expressed as arbitrary intensity units, measuring the integrated absorbance (IOD) as a formula that uses the sum of the negative log 10 of the intensity of the foreground pixels (IFi) divided by the intensity of the background pixels (IBi) [IOD = Σ^n − log (IFi/IBi)], n = total number of significant pixels, IFi = intensity of a significant pixel in the object on the foreground image, IBi = intensity of the corresponding pixel on the background image.

RESULTS

KLF6 Binds Cyclin D1. We have identified a cyclin E/A consensus-binding motif at the COOH terminus (amino acids 279–283) in KLF6. Within this motif is the sequence ZRXL, where Z and X are typically basic (23, 24). The NH_2 terminus of KLF6 contains a

number of leucine-rich repeats, including a highly conserved 11-residue stretch with the consensus sequence LxxLxLxxNxL that typically contributes to protein-protein interactions (25, 26). Taken together, these features suggested that KLF6 has the potential for protein-protein interactions, possibly binding one or more cyclins.

We tested binding to cyclins D1, E and A by coimmunoprecipitation assays after cDNA transfection of FLAG-KLF6 and the respective cyclins into 293T human embryonic kidney cells. These cells were chosen initially because of their undetectable levels of endogenous KLF6 and cyclin D1 protein, thus minimizing nonspecific background interactions. Only cyclin D1 coimmunoprecipitated with FLAG-tagged KLF6 (Fig. 1*A*). There was no specific binding of KLF6 to cyclins E or A under identical experimental conditions (data not shown). Specificity of binding was additionally confirmed in 293T cells by a reciprocal coimmunoprecipitation of human KLF6 with HA-tagged cyclin D1 (Fig. 1*A*).

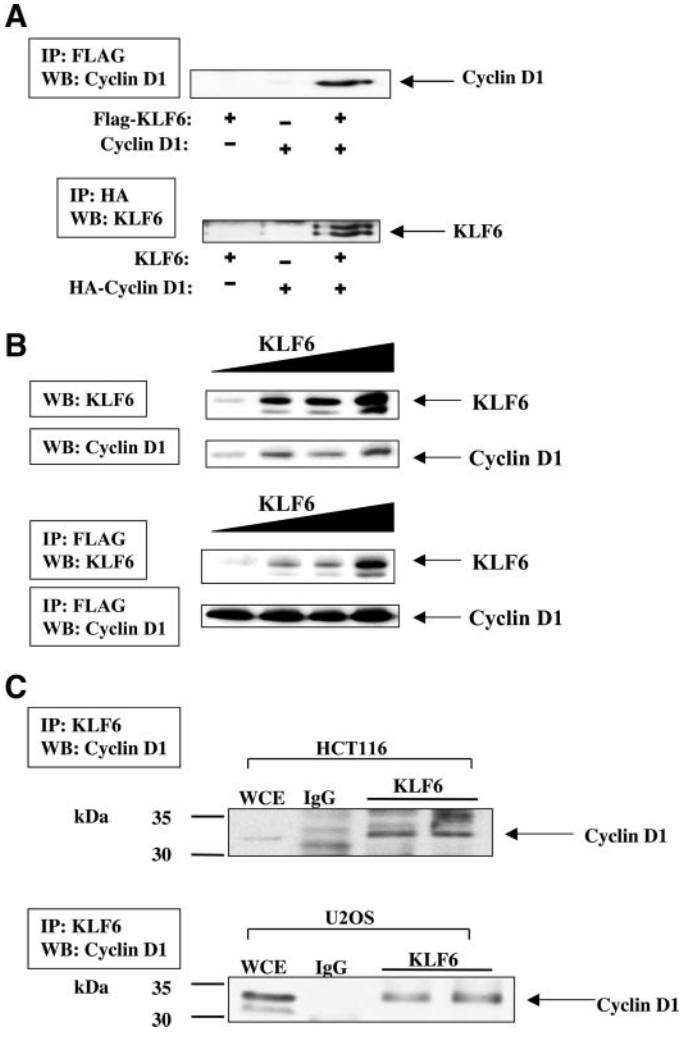

Fig. 1. Interaction between KLF6 and cyclin D1. *A*, FLAG-tagged KLF6 and cyclin D1 were cotransfected into 293T cells. Twenty-four h after transfection, FLAG-tagged KLF6 was immunoprecipitated (IP) using anti-FLAG antibody and anti-cyclin D1 was used for immunoblot. *Bottom panel*, HA-tagged cyclin D1 was immunoprecipitated by using anti-HA antibody. KLF6 was co-IP and detected by Western blot analysis ($n = 4$). *B*, concentration-dependent interaction between KLF6 and cyclin D1. *Top panel*, NIH3T3 cells stably expressing FLAG-tagged cyclin D1 were transfected with increasing concentrations of KLF6 (1–6 μg). Immunoblots of transfected KLF6 and endogenous cyclin D1 levels are shown. *Bottom panel*, following immunoprecipitation of cyclin D1 using anti-M2 FLAG agarose beads, Western blot analysis was performed to detect the levels of KLF6 co-IPed with cyclin D1 (IP/Western). *C*, endogenous interaction between KLF6 and cyclin D1 proteins. *Top panel*, KLF6 was IP from HCT116 whole cell extract (WCE) using anti-KLF6 antibody (2A2), and anti-cyclin D1 antibody was used for immunoblots showing co-IP of endogenous cyclin D1 with endogenous KLF6. *Bottom panel*, endogenous interaction between KLF6 and cyclin D1 in U2OS cells. IP with IgG was used as a control.

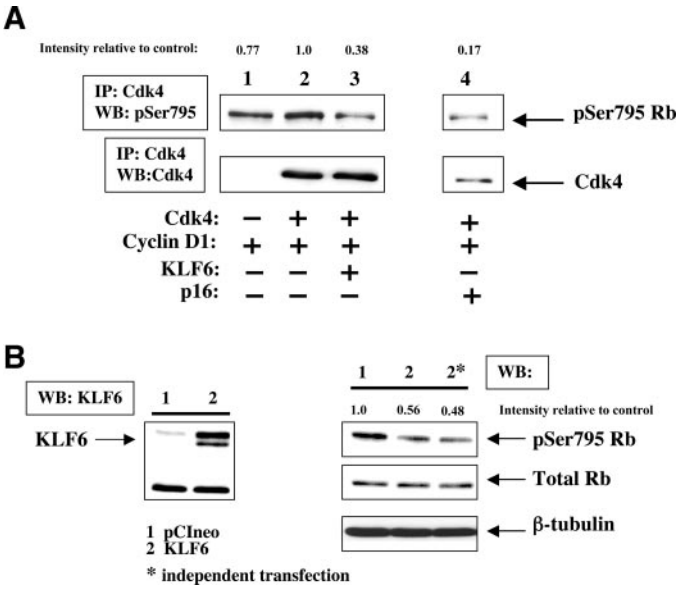

Fig. 2. KLF6 reduces Rb phosphorylation at Ser^{795}. *A*, cyclin D1 and cyclin-dependent kinase (cdk) 4 were cotransfected into HCT116 cells in the presence or absence of KLF6 or p16. cdk4 was immunoprecipitated from 500 μg of whole cell extract (WCE). Recombinant retinoblastoma (Rb) protein (0.5 μg) was added to the washed beads, and the reaction mixture was incubated in the presence of ATP for 30 min. at 30°C with gentle shaking. Samples were then subjected to Western blot analysis using antibody specific to the phosphorylated Ser^{795} form of Rb. Rb phosphorylation at Ser^{795} was quantitated by densitometry (in both *A* and *B*), and values are expressed in arbitrary intensity units relative to control (relative intensity unit = 1.0). The results shown are representative of three independent experiments. *B*, KLF6 was transfected into HCT116 cells and protein extracts were obtained 24 h after transfection for Western blot analysis of transfected KLF6 (*left*) and endogenous proteins (*right*). Overexpression of KLF6 results in reduced Rb phosphorylation at Ser^{795} *in vivo*.

Moreover, we demonstrate that KLF6 interacts with cyclin D1 in a dose-responsive manner. Using NIH3T3 cells that stably express FLAG-tagged cyclin D1, KLF6 was ectopically expressed by transient transfection at incremental concentrations. Twenty-four h after transfection, whole cell extracts were prepared and subjected to IP-Western blot analysis to assess KLF6-cyclin D1 binding. Cyclin D1 was immunoprecipitated using anti-M2-FLAG agarose beads. As shown in Fig. 1*B*, KLF6 was co-immunoprecipitated with cyclin D1 in a dose-responsive manner, corroborating binding specificity.

The physiological nature of the KLF6-cyclin D1 interaction was supported by evidence of binding between endogenous KLF6 and cyclin D1 proteins in HCT116 (colon carcinoma; Fig. 1*C*, *top panel*) and U2OS osteosarcoma cells (Fig. 1*C*, *bottom panel*) [additionally validated in Hep3B (hepatocellular carcinoma) and NIH3T3 cells; data not shown]. For each cell type, whole cell extracts were harvested 24 h after cells were seeded, and endogenous KLF6 protein was immunoprecipitated using a mouse monoclonal antibody specific to KLF6. Binding of endogenous cyclin D1 was detected by Western blot analysis as indicated in Fig. 1*B*. Immunoprecipitations using nonimmune rabbit immunoglobulin (IgG) was used as a control for binding specificity.

KLF6 Inhibits Cyclin D1/cdk4 Activity. We next examined whether the binding of KLF6 to cyclin D1 was associated with decreased cyclin D1 kinase activity. Cyclin D1/cdk4 complexes phosphorylate Rb at Ser^{795} (S795; Ref. 21). Thus, disruption of this interaction by KLF6 should lead to reduced phosphorylation of Rb-S795. HCT116 (colon cancer) cells that lack functional p16^{INK4a}, the prototypical cdk4 kinase inhibitor, were used in these experiments to avoid background inhibition of Rb phosphorylation by p16^{INK4a}. *In*

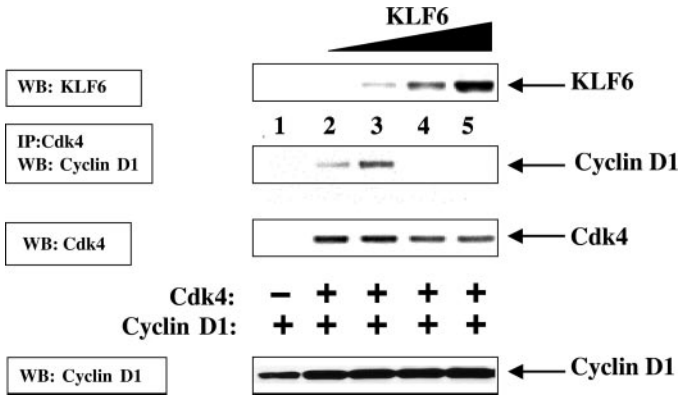

Fig. 3. Concentration-dependent disruption of cyclin D1/cyclin-dependent kinase (cdk) 4 complexes by KLF6. Cyclin D1 and cdk 4 were cotransfected into HCT116 cells at fixed amounts of DNA (5 μg) in the presence of increasing concentrations of transfected KLF6. Following immunoprecipitation of transfected cdk4, Western blot analysis was performed to detect the levels of cyclin D1 co-immunoprecipitated (co-IP) with cdk4 (IP/Western). Immunoblots of transfected KLF6 and cyclin D1 are also shown.

vitro nonradioactive cdk4 immunoprecipitation kinase assays were initially performed to assess Rb phosphorylation of Ser^{795} in the presence or absence of either KLF6 or p16^{INK4a} (positive control for cdk4 inhibition). As shown in Fig. 2, expression of KLF6 reduced Rb phosphorylation at S795 (Fig. 2*A*, *Lane 3*), paralleling the effect of the established tumor suppressor and CKI p16^{INK4a} (Fig. 2*A*, *Lane 4*). Of note, for proteins resolved on 12% SDS-PAGE, the Rb S795 antibody detects a single species on Western blot rather than the characteristic smear of multiple Rb isoforms that appears when using an antibody that detects total (*i.e.*, phosphorylated and unphosphorylated) Rb isoforms.

To validate the physiological nature of this finding, we assessed the effect of transfected KLF6 on the endogenous Rb protein in HCT116 cells (Fig. 2*B*) that express high levels of endogenous Rb protein. Compared with vector-transfected cells, KLF6-transfected cells expressed lower levels of endogenous S795 phosphorylated Rb (Fig. 2*B*).

KLF6 Reduces Binding of Cyclin D1 to cdk4. The interaction of KLF6 with cyclin D1 raised the interesting possibility that KLF6 function might resemble that of the p16^{INK4a} tumor suppressor in its relationship to cell cycle regulation. The p16^{INK4a} protein has been identified as a prototypical CKI that abrogates the kinase activity of cdk4 (12). This occurs by binding of p16 to cdk4, altering cyclin D1 binding and disrupting the binary cdk-cyclin complex. Consequently, the cyclin D1-cdk4 complex is inactivated and in turn results in reduced phosphorylation of the retinoblastoma tumor suppressor protein Rb, the classical substrate of the cyclin D1/cdk4 complex (21, 27, 28).

Having identified an interaction between KLF6 and cyclin D1, we examined whether KLF6, as with p16, could disrupt cyclin D1/cdk4 holoenzymes by binding to cyclin D1. Cyclin D1 and cdk4 were cotransfected into HCT116 in the presence of increasing concentrations of KLF6 (0–5 μg). Following immunoprecipitation of ectopic cdk4, transfected cyclin D1 protein was coimmunoprecipitated and quantified by immunoprecipitation/Western analysis. At increasing levels of KLF6 expression, reduced association between cyclin D1 and cdk4 was detected (Fig. 3), suggesting that increasing concentrations of KLF6 disrupt the cyclin D1/cdk4 holoenzyme.

Silencing of KLF6 Expression by siRNA Leads to Increased Cyclin D1 Binding to cdk4. If there is a direct relationship between KLF6 expression and Rb phosphorylation at Ser^{795}, then diminished levels of KLF6 should lead to increased cdk4 binding to cyclin D1 and increased phospho-Rb. We tested this prediction by assessing Rb phosphorylation following silencing of endogenous KLF6 mRNA using RNA interference. KLF6-specific siRNA (see "Materials and Methods") was expressed after transient transfection into HCT116 cells to determine the impact of silencing endogenous KLF6 on cyclin D1-cdk4 complex formation. For these experiments, cdk4 alone was ectopically expressed by transient transfection, and its interaction with endogenous cyclin D1 was assessed by immunoprecipitation from whole cell extracts, as shown in Fig. 4*A*. Following immunoprecipitation of cdk4, its complex formation with endogenous cyclin D1 was increased when endogenous KLF6 was reduced by specific siRNA. In other words, in the presence of markedly reduced levels of KLF6 protein, increased levels of cyclin D1/cdk4 holoenzymes were detected.

The biological effects of silencing endogenous KLF6 by siRNA were most pronounced in PC3 prostate cancer cells. PC3 cells are characterized by high transfection efficiency relative to HCT116 cells (as assessed by fluorescence-activated cell sorting analysis of green fluorescent protein-transfected cells; data not shown). Moreover, PC3 cells express reduced levels of endogenous KLF6 protein in comparison to HCT116 cells. Thus, PC3 cells were used to obtain higher

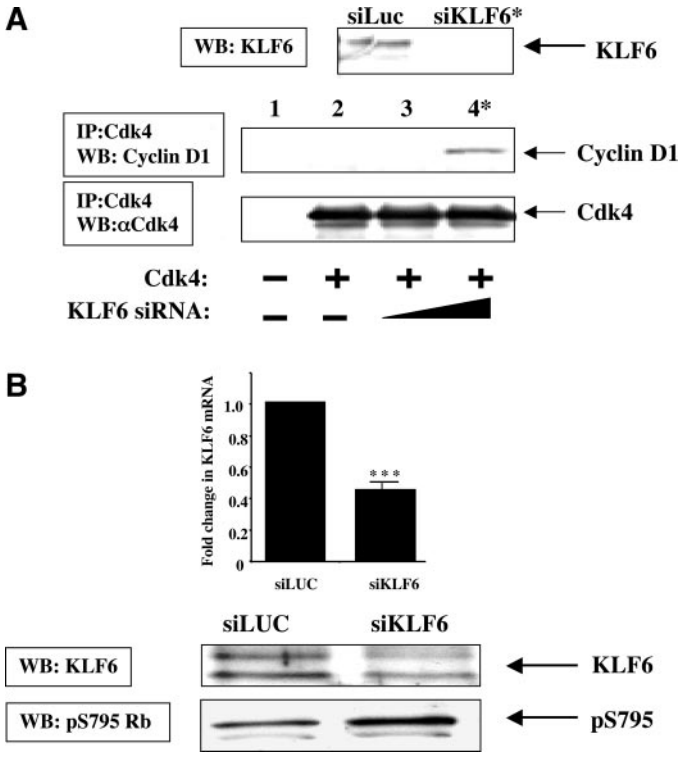

Fig. 4. Silencing of endogenous KLF6 by small interference RNA (siRNA) restores binding of endogenous cyclin D1 to cdk4 and reverses suppression by KLF6 of retinoblastoma (Rb) phosphorylation at Ser^{795}. *A*, *top*, a 19-nucleotide sequence of siRNA against KLF6 was cloned into the pSUPER plasmid (see "Materials and Methods"). The resulting pSUPER-KLF6 plasmid (siKLF6) was transfected into HCT116 cells and the pSUPER vector expressing an irrelevant protein, pSUPER-Luciferase (siLUC), was used as a control. Shown is an immunoblot of endogenous KLF6 protein levels in the presence or absence of transfected siKLF6 plasmid. *Bottom*, HCT116 cells were transfected with empty vector or cyclin-dependent kinase (cdk) 4 in the presence or absence of siKLF6. Twenty-four h after transfection, cells were harvested, and cdk4 was immunoprecipitated from whole cell extracts. An immunoblot of ectopically expressed cdk4 and endogenous cyclin D1 is shown. Silencing of KLF6 expression by siRNA (at the highest concentration denoted by an *asterisk*) increased detectable endogenous cyclin D1 binding to cdk4 as demonstrated by appearance of endogenous cyclin D1 that coimmunoprecipitates (co-IP) with cdk4 (*Lane 4*). *B*, siKLF6 was transfected into PC3 cells expressing markedly reduced endogenous KLF6 protein levels as shown in the KLF6 immunoblot. Silencing of endogenous KLF6 mRNA is confirmed by real-time quantitative PCR (see "Materials and Methods"). An immunoblot of pRb S795 shows that siKLF6 expression reverses suppression of Rb phosphorylation at Ser^{795} by KLF6 upon its targeted gene silencing. All data in this figure were derived from the same extracts and were reproducible in separate experiments.

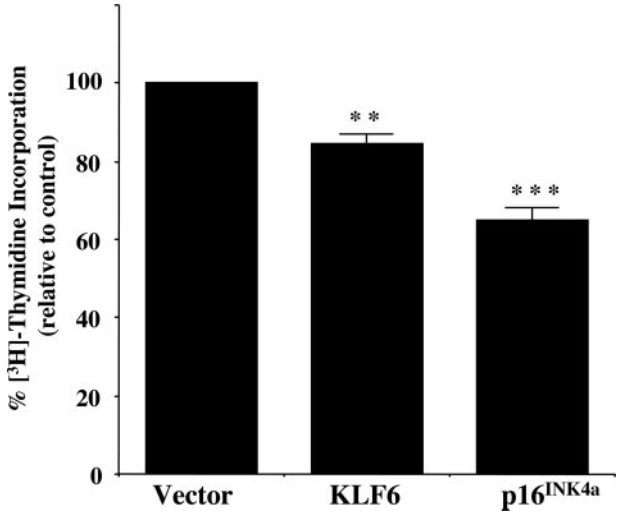

Fig. 5. KLF6 inhibits DNA synthesis in HCT116 colon cancer cells. Proliferation was estimated by measuring [^{3}H]thymidine incorporation into DNA. A total of 100–150 $\times$ 10^4 HCT116 cells were seeded in 12-well plates for transfection the next day with 1.6 μg of wild-type KLF6, p16^{INK4a}, or empty vector DNA as a control. Four to 6 h after transfection, cells were transferred to 10% FBS overnight, then starved for 24 h in 0.2% FBS. [^{3}H]Thymidine was added at 1 μCi/ml (1 μCi = 37 kBq) during the last 2 h of serum starvation. Disintegrations/min (dpm) were measured in a liquid scintillation counter. KLF6 has a statistically significant antiproliferative effect relative to expression vector alone (**, $P < 0.05$, two-way ANOVA, Bonferroni correction applied, $n = 5$). The effect of p16^{INK4a} is highly statistically significant (***, $P < 0.001$, two-way ANOVA, Bonferroni correction applied, $n = 4$) and may be due to lack of functional endogenous p16 in this cell line.

efficiency of KLF6 silencing to test the effect on Rb phosphorylation. As shown in Fig. 4*B*, we observed increased Rb phosphorylation at S795 as assessed by Western blot analysis upon KLF6 silencing in these cells.

KLF6 Inhibits Cell Proliferation and Promotes Growth Arrest in HCT116 Colon Carcinoma Cells. To assess whether KLF6 expression reduces proliferation of HCT116 cells, as previously shown in PC3 cells (1) that are also null for p16, DNA synthesis was determined by measuring [^{3}H]thymidine incorporation. A statistically significant inhibition of [^{3}H]thymidine incorporation in HCT116 cells was observed in the presence of wild-type KLF6 relative to empty vector control (Fig. 5).

To corroborate these results and to further study the impact of KLF6 on cell cycle distribution, we introduced KLF6 into HCT116 cells by retroviral infection. Western blot analysis (in HCT116 cells; Fig. 6*A*) and immunofluorescence (in U2OS cells chosen for their lowest background autofluorescence relative to either HCT116 or PC3 cells; Fig. 6*B*) confirmed KLF6 expression and nuclear localization upon transduction of KLF6.

Expression of KLF6, relative to pBabe empty vector control, led to a 50% increase of HCT116 cells in G_1 (Fig. 6*C*) with a concomitant decrease of cells in both S and G_2-M phases of the cell cycle. These results substantiated our observations obtained by [^{3}H]thymidine incorporation.

KLF6-Mediated Induction of p21 Results in Increased Redistribution of p21 to cdk2. Having established that KLF6 binds to cyclin D1, thereby inhibiting cyclin D-associated kinase activity, we next explored the effect of KLF6 on cdk2 complexes, as has been described for p16 (29–31). KLF6-mediated tumor suppression has been linked to its induction of the CKI, p21. Thus, we sought to correlate the effect of KLF6-mediated p21 induction and the redistribution of p21 to cdk2 as a result of KLF6 binding to cyclin D1. Retroviral expression of KLF6 stimulated the induction and redistribution of p21 on cdk2 complexes (Figs. 6 and 7). These findings are consistent with prior studies with keratinocytes in which p15 led to redistribution of Cip/Kip inhibitors from cdk4/6 to cdk2 (32, 33), including two independent studies demonstrating redistribution of p21 and/or p27 upon induction of p16 in U2OS cells (30, 34).

DISCUSSION

A key role of cyclin D1 is to bind cdk4 and form an active complex that can phosphorylate Rb. The Rb protein or the gatekeeper of the G_1-S transition (also referred to as the restriction point) is active when hypophosphorylated. Hypophosphorylated Rb blocks the transcriptional activity of E2F and represses genes involved in S-phase progression. Rb phosphorylation is inactivating such that phosphorylated Rb can no longer bind its corepressor E2F, allowing transcription of growth stimulatory genes and progression of cells from G_1 into S phase (35, 36).

Inhibition of cyclin D1/cdk4 occurs through interactions with cdk regulatory proteins of which there are two categories—the INK4 family (p16, p15, p18, and p19) that solely inhibit cdk4/6 kinase activity and the more promiscuous Cip/Kip family (p21, p27 and p57) that inhibit a broader range of cyclin–cdks in a concentration-dependent manner (37). For example, the p21 family of proteins enhances cyclin D1 kinase activity at low concentrations and inhibits this activity at high concentrations (38, 39). Of the INK4 family of CKIs, overexpression of the tumor suppressor p16 has been shown to reduce cyclin D1 holoenzyme levels and to cause G_1 cell cycle arrest as has been shown for CKIs identified to date (40–42).

Approximately 90% of human neoplasms have abnormalities in some component of the Rb pathway, with detectable lesions identified in either INK4a, cyclin D1, or Rb (43). Hyperactivation of cdks, overexpression of cyclins, or down-regulation of inhibitory factors such as the CKIs promote deregulated S-phase progression and loss of the G_1 checkpoint (37).

Having identified a physiological interaction between the tumor suppressor KLF6 and cyclin D1 (Fig. 1), we tested the hypothesis that KLF6 functions as a CKI via its interaction with cyclin D1. The tumor suppressor protein and prototypical CKI p16 functions by binding to cdk4 and disrupting cyclin D1/cdk4 complexes. Similarly, the KLF6 protein reduces cyclin D1/cdk4 complexes via its interaction with cyclin D1 (Fig. 3). Conversely, silencing the endogenous KLF6 gene by KLF6-specific siRNAs results in increased cyclin D1/cdk4 complexes as detected by immunoprecipitation-Western analysis (Fig. 4*A*).

We examined the biological consequences of these interactions in relation to the Rb pathway, testing phosphorylation of Rb at S795, a residue specifically phosphorylated by the cyclin D1/cdk4 complex (28). Expression of wild-type KLF6 resulted in reduced Rb phosphorylation at this site (Fig. 2). Moreover, when the wild-type function of KLF6 is eliminated by posttranscriptional gene silencing, phosphorylation of Rb at S795 is increased relative to wild-type KLF6 expression (Fig. 4*B*).

Taken together, the data support the hypothesis that KLF6 function resembles that of the tumor suppressor p16. Because p16 is nonfunctional in the cell lines chosen—HCT116 cells (44) PC3 and U2OS cells—it is possible that lack of p16, which normally disrupts cyclin D1/cdk4 complexes, potentiates the effect of wild-type KLF6 on cdk activity and accentuates the consequences of silencing endogenous KLF6 expression on cyclin D1/cdk4 holoenzyme formation.

The Cip/Kip family of CKIs has an additional function at low concentrations that includes promoting cyclin/cdk assembly (38, 39). Indeed, at low concentrations, the Cip/Kip family member, p21, stabilizes cyclin D1/cdk4 complexes and promotes cdk4 kinase activity (39, 45). Interestingly, as shown in Fig. 3, incremental expression

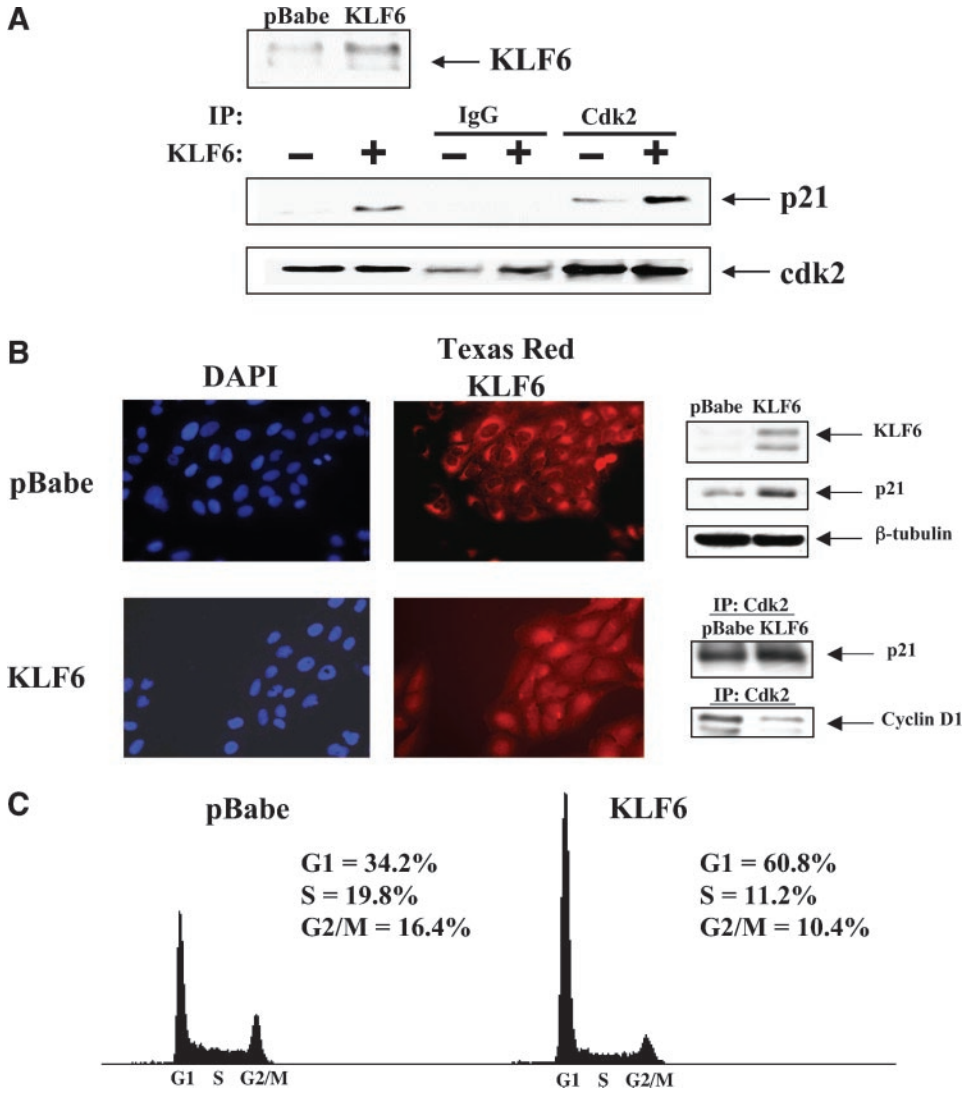

Fig. 6. Retroviral KLF6 expression increases p21 protein levels, forces the redistribution of p21 toward cyclin-dependent kinase (cdk) 2, and blocks S-phase entry in HCT116 cells. *A*, KLF6 or pBabe empty vector control were expressed by retroviral infection in HCT116 cells. Thirty-six h after infection, cells were harvested and processed for immunoprecipitation Western blot analysis of cdk2 and co-IP p21. Immunoblots for straight Westerns of KLF6, p21, and cdk2 are also shown. *B*, *Left panel*, immunofluorescence analysis of KLF6 localization in stably expressing pBabe or KLF6 osteosarcoma U2OS cells. 4′,6-Diamidino-2-phenylindole nuclear staining (*blue*); Zf9 rabbit polyclonal antibody directed against KLF6 (Texas Red-conjugated second antibody (*red*); mouse monoclonal antibody directed against cyclin D1 (FITC-conjugated second antibody; *green*). *Right panel*, immunoblots of KLF6, p21, and β-tubulin protein levels in osteosarcoma U2OS cells expressing pBabe control or KLF6. Increased binding of p21 to immunoprecipitated cdk2 in the presence of KLF6 is confirmed in U2OS cells, corroborating results obtained in HCT116 colon carcinoma cells (*A*). *C*, flow cytometric analyses of HCT116 cells were also performed 36 h after retroviral infection of either pBabe vector control or pBabe-KLF6. Cells were stained with propidium iodide, and DNA content was analyzed by flow cytometry. A total of 10,000 cells was analyzed in each experiment.

of KLF6 by transient transfection similarly suggests that at low concentrations KLF6 promotes cyclin D1/cdk4 complexes but disrupts them at higher concentrations. It is possible, therefore, that KLF6 functions in a concentration-dependent manner, as demonstrated for the CKI p21.

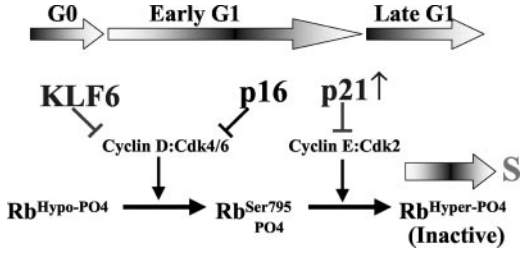

Fig. 7. Model of KLF6 and p16 inhibition of cyclin/cyclin-dependent kinase (cdk) complexes and the regulation of retinoblastoma (Rb) phosphorylation. Growth factor stimulation activates cyclin D-cdk4/6 activity, driving cells out of G_0 into G_1. Cyclin D1-cdk4/6 complex phosphorylates Rb at Ser^{795} and catalyzes the hyperphosphorylation of Rb upon the activation of cyclin E-cdk2 complexes in late G_1. Hyperphosphorylation of Rb causes the release of E2Fs to activate transcription of S-phase target genes (denoted by 'S'). KLF6 and p16 target the cyclin D-cdk4 complex, inhibiting phosphorylation of Rb at Ser^{795}. The up-regulation of p21 is an additional mechanism by which KLF6 can inhibit cell proliferation. When either KLF6 or p16 inhibits the cyclin D1/cdk4 complex, forced redistribution of p21 inactivates cyclin E-cdk2 complexes, thus preventing further inactivation of Rb by hyperphosphorylation.

As a tumor suppressor, the ability of KLF6 to transcriptionally up-regulate p21 (1) may not be mutually exclusive from its ability to physically interact with the cyclin D1 oncogene. Indeed, a number of growth suppressive mechanisms can be simultaneously triggered upon tumor suppressor activation. For example, p53-mediated apoptosis is triggered both by transcription-dependent (*e.g.*, up-regulation of bax, GADD45) and transcription-independent pathways (46). Expression of KLF6 by transient retroviral infection in HCT116 cells induces expression of the p21 CKI. Furthermore, as has been shown for the binding of p16 to cdk4, KLF6 expression results in the forced redistribution of p21 toward cdk2 complexes, likely enhanced by KLF6 binding to and catalytic inhibition of cyclin D1-cdk4 complexes in HCT116 cells. Thus, KLF6 targets cyclin/cdks from two converging KLF6-mediated growth suppressive pathways—binding and disruption of cyclin D1-cdk4 holoenzyme, coupled to induction and titration of p21 onto cdk2 complexes (Fig. 7).

Regulation of cell growth by KLF6 was demonstrated after its transient transfection in HCT116 colon cancer cells leading to inhibition of DNA synthesis (>15%), as well as G_1-S arrest after retroviral infection in these cells. Because HCT116 colon cancer cells are null for the prototypical CKI and tumor suppressor protein p16, these cells were used as a control to confirm effects on Rb phosphorylation and [^{3}H]thymidine incorporation. A greater inhibition in [^{3}H]thymi-

dine incorporation (~35%) in the presence of overexpressed exogenous p16 might be explained by HCT116's p16-null background, wherein its reintroduction has a more profound effect on DNA synthesis. Because HCT116 cells express relatively higher levels of endogenous KLF6 protein in comparison with PC3 (prostate cancer) as well as other colon cancer cell lines tested (1, 2), the effects of KLF6 overexpression might be more pronounced (or equal to that of p16) in a KLF6-null background.

In summary, our studies provide an additional mechanism of growth suppression by KLF6, which combined with its ability to induce p21, highlights its potential role in the complex regulatory network of cell cycle progression. These findings could have broader implications for further understanding mechanisms of growth dysregulation in human cancer(s) where KLF6 is inactivated.

ACKNOWLEDGMENTS

We thank Charles J. Sherr (St. Jude Children's Research Hospital) for providing the cyclin D1 plasmids and other cell cycle plasmids, Liliana Ossowski for important advice (Mount Sinai School of Medicine), and Garry Nolan (Stanford, CA) for providing the Phoenix A packaging cells. Carlos E. Alvarez provided assistance with densitometric analysis.

REFERENCES

1. Narla G, Heath KE, Reeves HL, et al. KLF6, a candidate tumor suppressor gene mutated in prostate cancer. Science (Wash. DC) 2001;294:2563–6.
2. Chen C, Hyytinen ER, Sun X, et al. Deletion, mutation, and loss of expression of KLF6 in human prostate cancer. Am J Pathol 2003;162:1349–54.
3. Reeves HL, Narla G, Oginbiyi O, et al. Kruppel-like Factor 6 (KLF6) is a tumor suppressor gene frequently inactivated in colorectal cancer. Gastroenterology. In press 2004.
4. Jeng YM, Hsu HC. KLF6, a putative tumor suppressor gene, is mutated in astrocytic gliomas. Int J Cancer 2003;105:625–9.
5. Yamashita K, Upadhyay S, Osada M, et al. Pharmacologic unmasking of epigenetically silenced tumor suppressor genes in esophageal squamous cell carcinoma. Cancer Cell 2002;2:485–95.
6. Bieker JJ. Kruppel-like factors: three fingers in many pies. J Biol Chem 2001;276:34355–8.
7. Black AR, Black JD, Azizkhan-Clifford J. Sp1 and Kruppel-like factor family of transcription factors in cell growth regulation and cancer. J Cell Physiol 2001;188:143–60.
8. Wang XW, Harris CC. TP53 tumour suppressor gene: clues to molecular carcinogenesis and cancer therapy. Cancer Surv 1996;28:169–96.
9. Crook T, Marston NJ, Sara EA, Vousden KH. Transcriptional activation by p53 correlates with suppression of growth but not transformation. Cell 1994;79:817–27.
10. Agarwal ML, Agarwal A, Taylor WR, Stark GR. p53 controls both the G_2-M and the G_1 cell cycle checkpoints and mediates reversible growth arrest in human fibroblasts. Proc Natl Acad Sci USA 1995;92:8493–7.
11. Shapiro GI, Edwards CD, Rollins BJ. The physiology of p16(INK4A)-mediated G_1 proliferative arrest. Cell Biochem Biophys 2000;33:189–97.
12. Ortega S, Malumbres M, Barbacid M. Cyclin D-dependent kinases, INK4 inhibitors and cancer. Biochim Biophys Acta 2002;1602:73–87.
13. Hall M, Peters G. Genetic alterations of cyclins, cyclin-dependent kinases, and Cdk inhibitors in human cancer. Adv Cancer Res 1996;68:67–108.
14. Collecchi P, Santoni T, Gnesi E, et al. Cyclins of phases G_1, S, and G_2-M are overexpressed in aneuploid mammary carcinomas. Cytometry 2000;42:254–60.
15. Hosokawa Y, Arnold A. Cyclin D1/PRAD1 as a central target in oncogenesis. J Lab Clin Med 1996;127:246–52.
16. Wang TC, Cardiff RD, Zukerberg L, Lees E, Arnold A, Schmidt EV. Mammary hyperplasia and carcinoma in MMTV-cyclin D1 transgenic mice. Nature (Lond.) 1994;369:669–71.
17. Yu Q, Geng Y, Sicinski P. Specific protection against breast cancers by cyclin D1 ablation. Nature (Lond.) 2001;411:1017–21.
18. Weinstein IB. Disorders in cell circuitry during multistage carcinogenesis: the role of homeostasis. Carcinogenesis (Lond.) 2000;21:857–64.
19. Ratziu V, Lalazar A, Wong L, et al. Zf9, a Kruppel-like transcription factor upregulated *in vivo* during early hepatic fibrosis. Proc Natl Acad Sci USA 1998;95:9500–5.
20. Jinno S, Hung SC, Yamamoto H, Lin J, Nagata A, Okayama H. Oncogenic stimulation recruits cyclin-dependent kinase in the cell cycle start in rat fibroblast. Proc Natl Acad Sci USA 1999;96:13197–202.
21. Grafstrom RH, Pan W, Hoess RH. Defining the substrate specificity of cdk4 kinase-cyclin D1 complex. Carcinogenesis (Lond.) 1999;20:193–8.
22. Brummelkamp TR, Bernards R, Agami R. A system for stable expression of short interfering RNAs in mammalian cells. Science (Wash. DC) 2002;296:550–3.
23. Adams PD, Li X, Sellers WR, et al. Retinoblastoma protein contains a C-terminal motif that targets it for phosphorylation by cyclin-cdk complexes. Mol Cell Biol 1999;19:1068–80.
24. Schulman BA, Lindstrom DL, Harlow E. Substrate recruitment to cyclin-dependent kinase 2 by a multipurpose docking site on cyclin A. Proc Natl Acad Sci USA 1998;95:10453–8.
25. Kobe B, Deisenhofer J. Crystal structure of porcine ribonuclease inhibitor, a protein with leucine-rich repeats. Nature (Lond.) 1993;366:751–6.
26. Kobe B, Kajava AV. The leucine-rich repeat as a protein recognition motif. Curr Opin Struct Biol 2001;11:725–32.
27. Boylan JF, Sharp DM, Leffet L, Bowers A, Pan W. Analysis of site-specific phosphorylation of the retinoblastoma protein during cell cycle progression. Exp Cell Res 1999;248:110–4.
28. Connell-Crowley L, Harper JW, Goodrich DW. Cyclin D1/Cdk4 regulates retinoblastoma protein-mediated cell cycle arrest by site-specific phosphorylation. Mol Biol Cell 1997;8:287–301.
29. Mitra J, Dai CY, Somasundaram K, et al. Induction of p21(WAF1/CIP1) and inhibition of Cdk2 mediated by the tumor suppressor p16(INK4a). Mol Cell Biol 1999;19:3916–28.
30. Jiang H, Chou HS, Zhu L. Requirement of cyclin E-Cdk2 inhibition in p16(INK4a)-mediated growth suppression. Mol Cell Biol 1998;18:5284–90.
31. Grimison B, Langan TA, Sclafani RA. p16Ink4a tumor suppressor function in lung cancer cells involves cyclin-dependent kinase 2 inhibition by Cip/Kip protein redistribution. Cell Growth Differ 2000;11:507–15.
32. Reynisdottir I, Polyak K, Iavarone A, Massague J. Kip/Cip and Ink4 Cdk inhibitors cooperate to induce cell cycle arrest in response to TGF-β. Genes Dev 1995;9:1831–45.
33. Reynisdottir I, Massague J. The subcellular locations of p15(Ink4b) and p27(Kip1) coordinate their inhibitory interactions with cdk4 and cdk2. Genes Dev 1997;11:492–503.
34. McConnell BB, Gregory FJ, Stott FJ, Hara E, Peters G. Induced expression of p16(INK4a) inhibits both CDK4- and CDK2-associated kinase activity by reassortment of cyclin-CDK-inhibitor complexes. Mol Cell Biol 1999;19:1981–9.
35. Harbour JW, Dean DC. The Rb/E2F pathway: expanding roles and emerging paradigms. Genes Dev 2000;14:2393–409.
36. Stevaux O, Dyson NJ. A revised picture of the E2F transcriptional network and RB function. Curr Opin Cell Biol 2002;14:684–91.
37. Mani S, Wang C, Wu K, Francis R, Pestell R. Cyclin-dependent kinase inhibitors: novel anticancer agents. Expert Opin Investig Drugs 2000;9:1849–70.
38. Sherr CJ, Roberts JM. CDK inhibitors: positive and negative regulators of G_1-phase progression. Genes Dev 1999;13:1501–12.
39. Cheng M, Olivier P, Diehl JA, et al. The p21(Cip1) and p27(Kip1) CDK 'inhibitors' are essential activators of cyclin D-dependent kinases in murine fibroblasts. EMBO J 1999;18:1571–83.
40. Quelle DE, Zindy F, Ashmun RA, Sherr CJ. Alternative reading frames of the INK4a tumor suppressor gene encode two unrelated proteins capable of inducing cell cycle arrest. Cell 1995;83:993–1000.
41. Quelle DE, Cheng M, Ashmun RA, Sherr CJ. Cancer-associated mutations at the INK4a locus cancel cell cycle arrest by p16INK4a but not by the alternative reading frame protein p19ARF. Proc Natl Acad Sci USA 1997;94:669–73.
42. Pestell RG, Albanese C, Reutens AT, Segall JE, Lee RJ, Arnold A. The cyclins and cyclin-dependent kinase inhibitors in hormonal regulation of proliferation and differentiation. Endocr Rev 1999;20:501–34.
43. Sherr CJ. Cancer cell cycles. Science (Wash. DC) 1996;274:1672–7.
44. Myohanen SK, Baylin SB, Herman JG. Hypermethylation can selectively silence individual p16ink4A alleles in neoplasia. Cancer Res 1998;58:591–3.
45. LaBaer J, Garrett MD, Stevenson LF, et al. New functional activities for the p21 family of CDK inhibitors. Genes Dev 1997;11:847–62.
46. Oesterreich S, Fuqua SA. Tumor suppressor genes in breast cancer. Endocr Relat Cancer 1999;6:405–19.